The PPh_3-Substituted Hydroxycyclopentadienyl Ruthenium Hydride [2,5-Ph_2-3,4-Tol_2(η^5-C_4COH)]Ru(CO)(PPh_3)H Is a More Efficient Catalyst for Hydrogenation of Aldehydes

Charles P. Casey,* Neil A. Strotman, Sharon E. Beetner, Jeffrey B. Johnson, David C. Priebe, Thomas E. Vos, Babak Khodavandi, and Ilia A. Guzei

Department of Chemistry, University of Wisconsin−Madison, Madison, Wisconsin 53706

Received November 1, 2005

The phosphine-substituted hydroxycyclopentadienyl ruthenium hydride [2,5-Ph_2-3,4-Tol_2(η^5-C_4COH)]-Ru(CO)(PPh_3)H (**8**) displayed behavior significantly different from that of the dicarbonyl analogue, including the failure to form an unreactive diruthenium complex analogous to the Shvo catalyst **5**. Complex **8** shows no apparent reduction of aldehydes in the absence of a trap but exchanges deuterium between the hydride of **8-RuDOD** and the aldehydic hydrogen of *p*-tolualdehyde. This provides evidence that aldehyde reduction by **8** occurs but is reversible. **8** catalyzes the hydrogenation of benzaldehyde under mild temperature and pressure conditions. A rate law of $-d[RCH{=}O]/dt = k[RCH{=}O][\mathbf{8}][H_2]^0$ was obtained.

Introduction

Recent advances in hydrogenation catalysts are revolutionizing carbonyl reduction chemistry. This wave of new research was initiated by Shvo's development of his hydroxycyclopentadienyl ruthenium hydride catalyst (**1**),[1] a species which utilizes electronically coupled acidic and hydridic hydrogens to efficiently catalyze the reduction of polar unsaturated species using hydrogen as the terminal reductant (Figure 1). Noyori has spearheaded the development of this new series of catalysts, terming the hydrogen cooperativity "ligand−metal bifunctional catalysis." Ru(arene)(diamine) (**2**) and Ru(BINAP)(diamine) (**3**) catalysts have become the most prominent members of this class, each capable of the reduction of ketones in high yields and enantioselectivities with over a million turnovers.[2−5] These catalysts utilize 2-propanol or hydrogen as the terminal reductant, providing "green" alternatives to stoichiometric reducing agents such as $LiAlH_4$ and $NaBH_4$.[6]

Computational studies on Noyori's Ru(*p*-cymene)(TsDPEN) catalyst (**2**) have indicated that the concerted transfer of the hydride and proton to carbonyls without prior coordination to the metal center is the lowest energy pathway for hydrogen transfer.[7] Our kinetic isotope effect observations on the tolyl analogue of Shvo's hydroxycyclopentadienyl ruthenium hydride

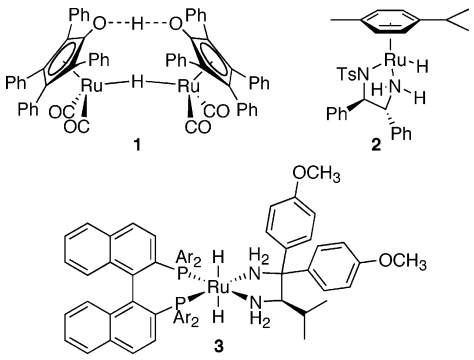

Figure 1. Ligand−metal bifunctional catalysts.

4 and on Noyori's catalyst **2** support the outer-sphere concerted transfer of hydrogen to carbonyl compounds and to imines (Figure 2).[8,9]

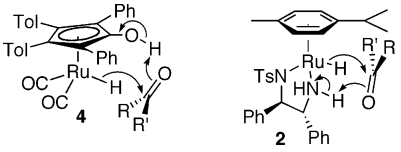

Figure 2. Concerted hydrogen transfer mechanism for ligand−metal bifunctional catalysts **2** and **4**.

Our detailed kinetic studies, which provided accurate activation parameters for each step of the Shvo catalytic system, have enabled simulation of the overall rate of the Shvo catalytic cycle and of the relative concentrations of the ruthenium species present during catalysis (Scheme 1).[10] Due to the reactive nature of the two species directly involved in the catalytic cycle (ruthenium hydride **4** and the oxidized, coordinatively unsaturated intermediate **A**), the most stable species in the Shvo catalytic system is the diruthenium bridging hydride **5**, which

* To whom correspondence should be addressed. E-mail: casey@chem.wisc.edu.

(1) (a) Shvo, Y.; Czarkie, D.; Rahamim, Y.; Chodosh, D. F. *J. Am. Chem. Soc.* **1986**, *108*, 7400. (b) Menashe, N.; Shvo, Y. *Organometallics* **1991**, *10*, 3885. (c) Menashe, N.; Salant, E.; Shvo, Y. *J. Organomet. Chem.* **1996**, *514*, 97.

(2) (a) Haack, K.-J.; Hashiguchi, S.; Fujii, A.; Ikariya, T.; Noyori, R. *Angew. Chem., Int. Ed.* **1997**, *36*, 285. (b) Noyori, R.; Hashiguchi, S. *Acc. Chem. Res.* **1997**, *30*, 97. (c) Marsumura, K.; Hashiguchi, S.; Ikariya, T.; Noyori, R. *J. Am. Chem. Soc.* **1997**, *119*, 8738.

(3) Noyori, R.; Ohkuma, T. *Angew. Chem., Int. Ed.* **2001**, *40*, 40 and references therein.

(4) (a) Abdur-Rashid, K.; Faatz, M.; Lough, A. J.; Morris, R. H. *J. Am. Chem. Soc.* **2001**, *123*, 7473. (b) Abdur-Rashid, K.; Lough, A. J.; Morris, R. H. *Organometallics* **2001**, *20*, 1047. (c) Abdur-Rashid, K.; Clapham, S. E.; Hadzovic, A.; Harvey, J. N.; Lough, A. J.; Morris, R. H. *J. Am. Chem. Soc.* **2002**, *124*, 15104.

(5) For a recent review of hydrogenation of polar bonds catalyzed by ruthenium hydride complexes, see: Clapham, S. E.; Hadzovic, A.; Morris, R. H. *Coord. Chem. Rev.* **2004**, *248*, 2201.

(6) Fehring, V.; Selke, R. *Angew. Chem., Int. Ed.* **1998**, *37*, 1827.

(7) Yamakawa, M.; Ito, H.; Noyori, R. *J. Am. Chem. Soc.* **2000**, *122*, 1466.

(8) Casey, C. P.; Singer, S. W.; Powell, D. R.; Hayashi, R. K.; Kavana, M. *J. Am. Chem. Soc.* **2001**, *123*, 1090.

(9) Casey, C. P.; Johnson, J. B. *J. Org. Chem.* **2003**, *68*, 1998.

(10) Casey, C. P.; Johnson, J. B. Unpublished results.

10.1021/om0509387 CCC: $33.50
Publication on Web 01/25/2006

is in equilibrium with the active reducing agent **4** and coordinatively unsaturated **A**. At low temperatures, the rate of dissociation of **5** severely limits the overall rate of reduction. At high temperatures (>80 °C), the reversible dissociation to **5** becomes rapid enough to support efficient catalysis, but the unreactive diruthenium compound **5** still constitutes a large fraction of the ruthenium species.

Scheme 1

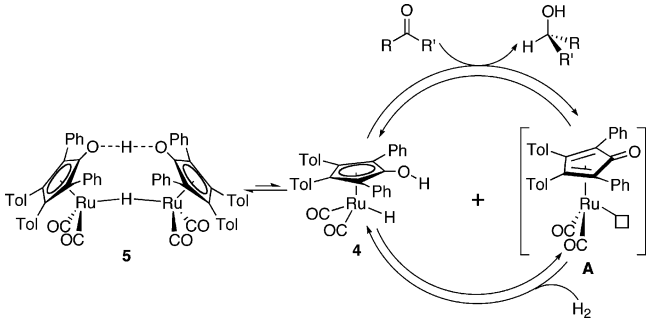

To develop more active ruthenium catalysts, we sought to minimize the amount of ruthenium present as an unreactive diruthenium hydride. Previously, we reported use of CpNHPh analogues that prevented dimerization but required acid catalysis for fast rates.[11] Here we report a promising alternative strategy involving replacement of a carbonyl with a phosphine ligand. Two benefits were anticipated from phosphine substitution: (1) the steric bulk of the phosphine was expected to destabilize the diruthenium bridging hydride, and (2) its electron-donating properties were expected to increase the hydride donor ability of the hydridic active species. In addition, the availability of large numbers of phosphines with varying steric and electronic properties provides many possibilities for future catalyst development.

Here we describe the preparation of a triphenylphosphine-substituted hydroxycyclopentadienyl ruthenium hydride catalyst, which does not form diruthenium bridging hydride species. We also report its activity as an aldehyde hydrogenation catalyst under mild conditions and discuss the catalytic cycle involved.

Results

[2,5-Ph$_2$-3,4-Tol$_2$(η^5-C$_4$COH)Ru(CO)(PPh$_3$)Cl] (7). Reaction of ruthenium chloride **6** with excess PPh_3 in refluxing THF for 4 days produced the corresponding triphenylphosphine-substituted ruthenium chloride complex **7** in 91% yield (Scheme 2). **7** was characterized by spectroscopy and by X-ray crystallography (Figure 3).

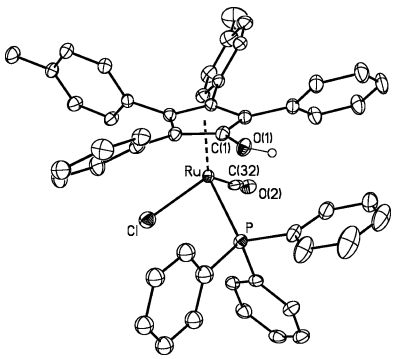

Figure 3. X-ray crystal structure of **7**. Selected bond lengths (Å) and angles (deg): Ru−P, 2.3423(13); P−Ru−Cl, 86.73(5); C(32)−Ru−Cl, 93.09(16); C(32)−Ru−P, 89.79(14); P−Ru−C(1)−O(1), 1.2(4); Cl−Ru−C(1)−O(1), 89.0(4).

Scheme 2

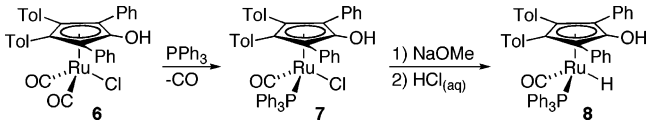

[2,5-Ph$_2$-3,4-Tol$_2$(η^5-C$_4$COH)Ru(CO)(PPh$_3$)H] (8). Reaction of the triphenylphosphine chloride complex **7** with sodium methoxide in refluxing methanol for 4 h led to the isolation of the phosphine-substituted ruthenium hydride complex **8** in 83% yield as an air-sensitive orange powder. In the ^{1}H NMR spectrum of **8**, a doublet (J_{HP} = 34.2 Hz) at δ −10.37 established the presence of a ruthenium hydride coupled to phosphorus. In the X-ray crystal structure of **8** (Figure 4), the bulky PPh_3 ligand lies directly below the hydroxyl group on the Cp ligand. The phosphine hydride complex **8** is significantly more air sensitive than the corresponding chloride complex **7**. Upon exposure to air, a solution of **8** decomposes within seconds to unidentified dark material.

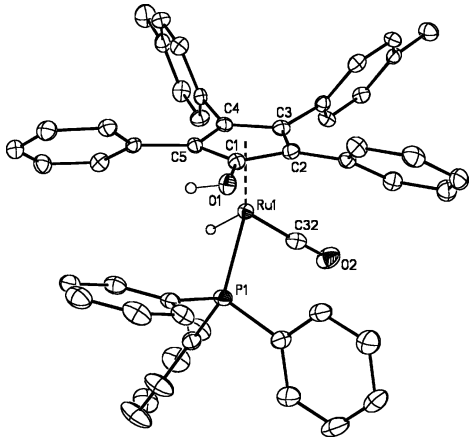

Figure 4. X-ray crystal structure of **8**. Selected bond lengths (Å) and angles (deg): Ru(1)−P(1), 2.2792(10); P(1)−Ru(1)−H(1), 81.6(13); C(32)−Ru(1)−H(1), 78.6(13); C(32)−Ru(1)−P(1), 88.18(13); P(1)−Ru(1)−C(1)−O(1), 8.9(3); C(32)−Ru(1)−C(1)−O(1), 90.0(4).

Acidity of PPh$_3$-Substituted Ruthenium Complexes. The acidity of the hydroxyl proton is vital to comparing the reactivity of phosphine-substituted ruthenium hydrides to that of the parent dicarbonyl complex **4**. The pK_a of the unsubstituted ruthenium hydride **4** was previously determined to be 17.5 in CH_3CN using Norton's IR method.[12] The same procedure was used to determine the pK_a values of the hydroxyl proton in the PPh_3-substituted chloride **7** (pK_a = 18.1) and hydride **8** (pK_a = 20.7). These phosphine-substituted complexes are significantly less acidic than the related dicarbonyl compounds (pK_a = 12.0 and 17.5, respectively). The diminished acidity influences the reactivity of **8** and may alter the mechanism of hydrogen transfer.

Loss of H_2 from **8** occurs more slowly than from dicarbonyl ruthenium hydride **4**, which loses H_2 upon heating at 80 °C for several hours. When the triphenylphosphine-substituted ruthenium hydride **8** (15 mM) was heated at 95 °C in toluene-d_8 under 200 Torr of CO for 72 h, ^{1}H NMR spectroscopy showed about 30% loss of H_2 from **8** and appearance of a resonance (δ

(11) Casey, C. P.; Vos, T. E.; Singer, S. W.; Guzei, I. A. *Organometallics* **2002**, *21*, 5038.

(12) (a) Jordan, R. F.; Norton, J. R. *J. Am. Chem. Soc.* **1982**, *104*, 1255. (b) Moore, E. J.; Sullican, J. M.; Norton, J. R. *J. Am. Chem. Soc.* **1986**, *108*, 2257.

1.90) consistent with the formation of the ruthenium dicarbonyl phosphine [2,5-Ph_2-3,4-Tol_2(η^4-C_4CO)]Ru($CO)_2$(PPh_3).

Exchange of Ruthenium Hydride with D_2. In contrast to the dicarbonyl ruthenium hydride **4**, which undergoes complete exchange of D_2 with RuH (but not with CpOH) within 1 h at room temperature,[13] the triphenylphosphine-substituted ruthenium hydride **8** showed no exchange of RuH with D_2 (4 atm) at room temperature over 48 h. When it was heated at 95 °C for 96 h, approximately 50% exchange of ruthenium hydride with D_2 was observed, which is similar to the rate of hydrogen loss (30% over 72 h).

Stoichiometric Aldehyde Reduction by 8. When the reaction of **8** with excess benzaldehyde in toluene-d_8 at room temperature was monitored by ^{1}H NMR spectroscopy, partial disappearance of the ruthenium hydride resonance (δ −10.37) and concurrent appearance of resonances due to benzyl alcohol (δ 4.30) were seen within 30 min, indicating that some reduction had occurred. However, little additional reduction was seen over the following 2 h, indicating that equilibrium was being approached. No bridging hydride resonances were observed, but new tolyl methyl resonances were seen at δ 1.61 and 1.81 for the ruthenium product **9**.

To isolate this new ruthenium complex (**9**), a large excess of benzaldehyde (>100 equiv) was added to a toluene solution of **8**. After several hours, solvent was evaporated and the crude product was washed with pentane to remove excess aldehyde and alcohol. The resulting yellow solid displayed two tolyl ^{1}H NMR resonances at δ 1.61 and 1.81.

Spectroscopy was little help in determining the structure of **9**. The absence of a hydride resonance eliminated a diruthenium bridging hydride as a possible structure. No resonances for coordinated benzaldehyde or coordinated benzyl alcohol were present. The largest fragment seen in the electrospray mass spectrum corresponded to (**8** − H)$^+$. IR spectroscopy showed the presence of only a single metal carbonyl stretching frequency at 1960 cm^{-1}, and ^{31}P NMR spectroscopy indicated only a single phosphine resonance at δ 52.4. ^{13}C NMR spectroscopy showed a resonance at δ 173.7, which is consistent with the carbonyl carbon of an η^4-dienone moiety.

At this point, we considered two possible structures for **9**, the unsaturated 16e dienone carbonyl triphenylphosphine complex [2,5-Ph_2-3,4-Tol_2(η^4-C_4CO)]Ru(PPh_3)(CO) (**B**) and its dimer **C**, analogous to the well-known dienone dicarbonyl dimer **10** (Figure 5). Since cis and trans isomers of dimer **C** are possible, four ^{1}H NMR tolyl resonances and two ^{31}P NMR resonances would have been expected. However, the possibility that only a single isomer formed could not be excluded. The electrospray mass spectrum would be compatible with dimer **C** if dissociation occurred during ionization. The monoruthenium nature of complex **9** was later established by PGSE NMR experiments (see the Supporting Information). At this point, we favored structure **B**, even though four-coordinate Ru(0) complexes are rare and are expected to be highly reactive.

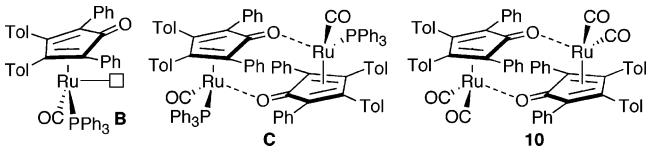

Figure 5.

(13) The mechanism of this exchange reaction is not well understood and is currently under investigation: Casey, C. P.; Johnson, J. B.; Singer, S. W.; Cui, Q. *J. Am. Chem. Soc.* **2005**, *127*, 3100.

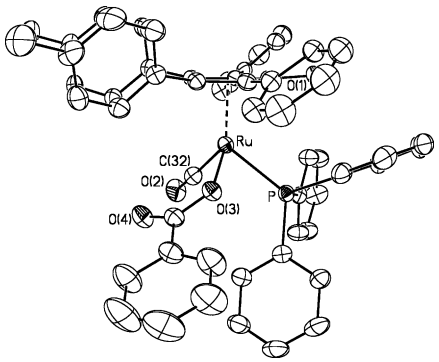

Figure 6. X-ray crystal structure of **9**. Selected bond lengths (Å) and angles (deg): Ru−P, 2.3362(14); C(32)−Ru−O(3), 97.49(18); O(3)−Ru−P, 84.52(11); C(32)−Ru−P, 87.73(16); P−Ru−C(1)−O(1), 3.1(4).

Scheme 3

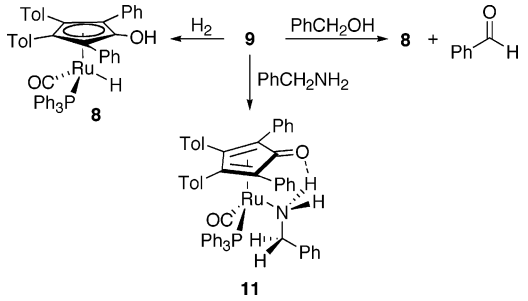

Chemical Characterization of Ruthenium Complex 9. As expected for a highly reactive four-coordinate Ru(0) complex such as **B**, the new complex **9** rapidly reacted with H_2, rapidly dehydrogenated alcohols, and rapidly reacted with benzylamine to produce the amine complex **11** (Scheme 3). When excess benzyl alcohol (0.311 M) was added to a solution of **9** (0.0105 M) in toluene-d_8, nearly complete conversion of **9** to ruthenium hydride **8** was observed within 10 min at room temperature. These products result from the microscopic reverse of reduction, the transfer of hydrogen from benzyl alcohol to the unsaturated species.

X-ray Crystal Structure of Reactive Complex 9. Eventually, a single crystal of the new complex **9** was obtained and, much to our surprise, X-ray crystallography showed that it was the benzoic acid adduct [2,5-Ph_2-3,4-Tol_2(η^5-C_4COH)]-Ru(O_2CPh)(PPh_3)(CO) (**9**) (Figure 6).

Since most of the yellow powder did not form crystals, we could not be sure that the bulk material was the same as that of the single crystals of **9**. In principle, ^{1}H NMR spectroscopy could distinguish between **9** and dienone **B** or dienone dimer **C** on the basis of the ratio of integrals for the aryl hydrogen and methyl hydrogen resonances (33:6 vs 38:6). However, due to the low solubility of the material, this was not a reliable technique. Unfortunately, neither ^{13}C NMR spectroscopy nor HRMS could distinguish between **9** and **B** either. The frequency of the carbon resonance at δ 173.7 is consistent with both a dienone carbonyl and a carboxylate carbonyl, while the exact mass obtained could be formulated as either [**B** + H]$^+$ or as [**9** − O_2CPh]$^+$.

Instead, we turned to making a similar derivative starting from *p*-tolualdehyde and **8**. If reduction of *p*-tolualdehyde by **8** gave a product with exactly the same spectral properties as from benzaldehyde, then a carboxylic acid complex could be ruled out as the bulk material. However, if a *p*-toluic acid adduct were formed, it would contain an additional methyl group which could

be easily observed by NMR spectroscopy. **8** was combined with a large excess (80 equiv) of *p*-tolualdehyde in toluene; after 24 h, the toluene was evaporated and the residue was washed with pentane to remove *p*-tolualdehyde and 4-methylbenzyl alcohol. The resulting yellow powder (**9-Me**) showed ^{1}H NMR resonances in CD_2Cl_2 for tolyl methyl groups at δ 2.06, 2.24, and 2.30 and for a hydroxyl proton at δ 3.68. ^{1}H NMR spectroscopy in CD_2Cl_2 showed that treatment of **9-Me** with H_2 produced **8** and *p*-toluic acid (δ 2.44).

This spectroscopic data established that **9-Me** is the *p*-toluic acid adduct [2,5-Ph_2-3,4-Tol_2(η^5-C_4COH)]Ru(O_2CTol)(PPh_3)(CO) (**9-Me**) and that the bulk material from the benzaldehyde reduction was the benzoic acid adduct **9**. We suggest that benzoic acid adduct **9** is formed during reduction of benzaldehyde by **8**, due to the presence of small amounts of benzoic acid in the excess benzaldehyde employed. The reduction of benzaldehyde by **8** produces the unsaturated reactive intermediate **B**, which is then trapped by benzoic acid to give **9** (Scheme 4).

Scheme 4

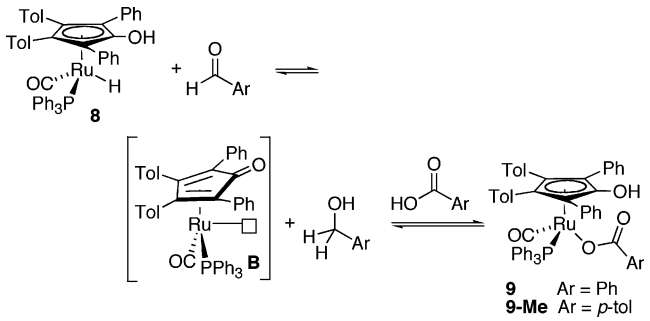

Previously, we reported the ruthenium dicarbonyl formate complex [2,5-Ph-3,4-Tol(η^5-C_4COH)]Ru($CO)_2$(O_2CH) (**12**),[14] which underwent rapid exchange with DCO_2H at −20 °C. This exchange was proposed to involve reversible formation of unsaturated intermediate **A** (Scheme 5). It seems likely that the reactions of **9** and **9-Me** with H_2 or alcohols involve fast, reversible dissociation of the carboxylic acid to give the unsaturated intermediate **B**, followed by reaction of H_2 or alcohol with **B** to form **8**.

Scheme 5

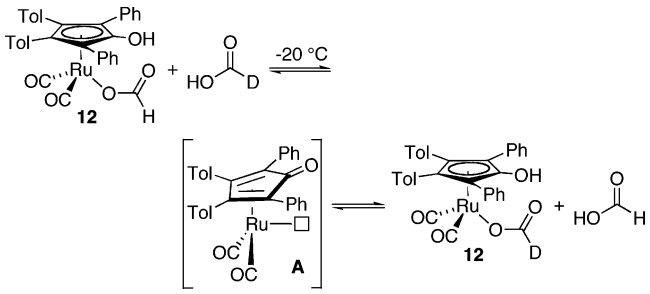

Stoichiometric Aldehyde Reduction by 8 in the Absence of a Carboxylic Acid. When an excess of freshly distilled *p*-tolualdehyde (<0.01% *p*-toluic acid) was added to a solution of **8** in CD_2Cl_2 or C_6D_6, no formation of 4-methylbenzyl alcohol was observed, even after 20 h. Addition of *p*-toluic acid led to rapid formation of 4-methylbenzyl alcohol and **9-Me**.

The failure to observe 4-methylbenzyl alcohol suggested either that an acid catalyst was necessary for aldehyde reduction or that reduction was reversible and thermodynamically unfavorable in the absence of a trap for unsaturated species **B**.

To test the hypothesis of reversible reduction, we monitored the reaction of *p*-tolualdehyde (0.215 M) with the dideuterated analogue [2,5-Ph_2-3,4-Tol_2(η^5-C_4COD)]Ru($CO)_2$D (**8-RuDOD**; 10.8 μM) in toluene-d_8 at 26 °C by ^{1}H NMR spectroscopy (Scheme 6). The hydride resonance of **8** grew in with a half-life of ∼25 min. The growth of the hydride resonance followed pseudo first-order kinetics; assuming second-order kinetics (vide infra) gave $k = 2.24 \times 10^{-3}$ M^{-1} s^{-1}. When the reaction of *p*-tolualdehyde (0.215 M) with the singly labeled isotopologue [2,5-Ph_2-3,4-Tol_2(η^5-C_4COH)]Ru($CO)_2$D (**8-RuDOH**) (10.8 μM), obtained by shaking **8-RuDOD** with H_2O, was monitored by ^{1}H NMR spectroscopy at 26 °C in toluene-d_8, the hydride resonance of **8** appeared with a half-life of ∼14 min ($k = 4.07 \times 10^{-3}$ M^{-1} s^{-1}).

Scheme 6

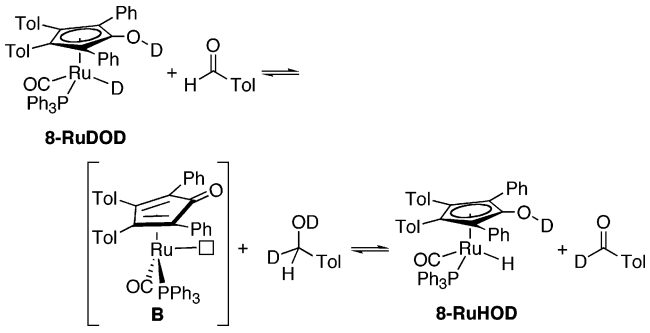

These isotope exchange experiments clearly demonstrate that **8** reduces aldehydes reversibly and that the equilibrium lies far on the side of **8** and the aldehyde, rather than **B** and alcohol, due to the inherent instability of the unsaturated 16e intermediate **B**. These isotope exchange experiments also provided an initial measure of the deuterium kinetic isotope effect for aldehyde reduction: $k_{OH}/k_{OD} = 1.8$.

Hydrogenation of Benzaldehyde Catalyzed by 8. Having observed reversible aldehyde reduction by **8**, we decided to investigate the catalytic hydrogenation of benzaldehyde. If H_2 trapped the unsaturated intermediate **B** and converted it back to hydride **8**, then aldehyde reduction would be possible. The hydrogenation of benzaldehyde (0.530 M) under 2.5 atm of H_2 in toluene-d_8 was catalyzed by **8** (18 mM, 3 mol %). ^{1}H NMR spectroscopy showed that disappearance of benzaldehyde followed a first-order decay and was completely converted to benzyl alcohol (29 turnovers) over 10 h at room temperature. The ruthenium hydride **8** was the only ruthenium compound observed during the course of the hydrogenation.

The hydrogenation of benzaldehyde (0.97 M) catalyzed by **8** (5.2−8.0 mM, 0.5−0.8 mol %) in toluene was also monitored in a high-pressure vessel (11−55 atm H_2) at 22 and 45 °C using in situ IR spectroscopy with a REACT-IR probe. The hydrogenations were followed by monitoring the disappearance of the benzaldehyde CO band at 1709 cm^{-1}. These reactions followed first-order decay of benzaldehyde and were complete in 5−20 h. Plots of ln [PhCHO] vs time were linear to over 90% reaction, indicating a first-order rate dependence on aldehyde and no inhibition by the product benzyl alcohol (see Supporting Information).

Table 1 shows the dependence of the rates of these catalytic hydrogenations on the concentration of **8** and on H_2 pressure. This process shows a first-order dependence on the catalyst concentration (entries 4−6) and essentially no dependence on

(14) Casey, C. P.; Singer, S. W.; Powell, D. R. *Can. J. Chem.* **2001**, *79*, 1002.

Table 1. Catalytic Hydrogenation of Benzaldehyde (0.97 M) in Toluene

entry	[**8**] (mM)	temp (°C)	pressure (atm)	k_{obs} (10^{-5} s^{-1})	k (10^{-3} M^{-1} s^{-1})
1	18.1	22	2.5[a]	12	6.7
2	8.0	22	35	5.6	7.0
3	5.5	45	11	16	29
4	5.2	45	35	16	31
5	7.2	45	35	21	29
6	8.0	45	35	23	29
7	5.9	45	55	18	31

[a] This hydrogenation of benzaldehyde (0.530 M) was carried out in a resealable NMR tube and monitored by ^{1}H NMR spectroscopy.

Scheme 7

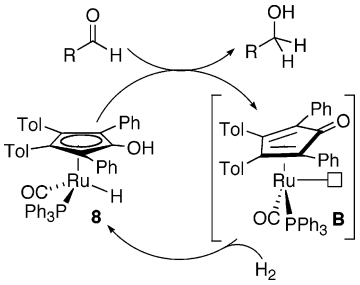

H_2 pressure over a wide range (entries 1 and 2; entries 3, 4, and 7). There is a moderate temperature dependence, and an increase of 23 °C produced a rate acceleration of ~4. Addition of benzoic acid gave rates of catalytic hydrogenation which were within experimental error of those obtained in the absence of benzoic acid.

These experiments established the rate law $-d[PhCHO]/dt = k_{obs}[PhCHO][H_2]^0 = k[\mathbf{8}][PhCHO][H_2]^0$. This rate law is consistent with the catalytic cycle shown in Scheme 7. Rate-limiting hydrogen transfer from **8** to the aldehyde produces the corresponding alcohol and the unsaturated intermediate **B**. Under the catalytic conditions, **B** reacts much more rapidly with H_2 than with alcohols to complete the catalytic cycle by regenerating **8**.

Hydrogenation of Propanal Catalyzed by 8. To evaluate the utility of catalyst **8** for hydrogenation of aliphatic aldehydes, the hydrogenation of propanal (1.358 M) with **8** (5.2 mM) in toluene at 45 °C under 35 atm of H_2 was followed by monitoring the aldehyde CO band at 1733 cm^{-1}. The disappearance of propanal followed first-order decay. Using the rate law established for hydrogenation of benzaldehyde with **8**, a rate constant of $k = 4.6 \times 10^{-2}$ M^{-1} s^{-1} was determined. Catalyst **8** hydrogenated propanal ~50% faster than it did benzaldehyde.

Imine Hydrogenation Catalyzed by 8. The hydrogenation of *N*-benzylideneaniline (PhN=CHPh) (0.252 M) under ~4 atm of H_2 in toluene-d_8 at 63 °C catalyzed by **8** (9.5 mM, 4 mol %) was monitored by ^{1}H NMR spectroscopy. The disappearance of imine (δ 8.09) followed pseudo first-order kinetics; a nonlinear least-squares fit of the plot of [imine] versus time gave $k_{obs} = 1.10 \pm 0.03 \times 10^{-5}$ s^{-1}; $k = (1.17 \pm 0.03) \times 10^{-3}$ M^{-1} s^{-1}. After 86 h, the reaction was complete (27 turnovers). Throughout the reaction, the only appreciable ruthenium species in solution was **8** (δ 1.87, 1.82) and there was no evidence for ruthenium amine complexes. However, ~29% catalyst decomposition to several unidentified products was seen. For comparison, the hydrogenation of benzaldehyde catalyzed by **8** at 45 °C ($k = 3.0 \times 10^{-2}$ M^{-1} s^{-1}) occurs ~26 times faster than imine hydrogenation at a temperature 18 °C higher.

Discussion

In an effort to develop a more active ruthenium hydrogenation catalyst related to the Shvo system, we sought to minimize the fraction of ruthenium present as an unreactive diruthenium hydride by adding a bulky triphenylphosphine ligand. This strategy produced a significantly different catalyst system in which ruthenium shuttles between hydride **8** and an unseen unsaturated intermediate **B** without the involvement of any unreactive diruthenium species.

No evidence for a phosphine-substituted diruthenium bridging hydride analogous to **5** was obtained in studies of the phosphine-substituted hydride **8**. In the all-carbonyl system, the unseen coordinatively unsaturated intermediate **A** either reacts with ruthenium hydride **4** to form the unreactive bridging hydride **5** or reacts with H_2 to re-form the monoruthenium hydride **4** (Scheme 1). In contrast, the phosphine-substituted coordinatively unsaturated intermediate **B** reacts only with H_2 to re-form ruthenium hydride **8** (Scheme 7). The steric bulk of the PPh_3 ligand is probably the crucial factor in destabilizing diruthenium species. As a consequence, the phosphine-substituted catalyst system does not have an unreactive sink for ruthenium and all the ruthenium is present as the active reducing agent **8**.

While no reduction of *p*-tolualdehyde by **8** was seen in the absence of a trap, isotopic exchange between ruthenium deuteride (**8-RuDOD**) and *p*-tolualdehyde provided evidence for reversible reduction. In the absence of a trap, the equilibrium lies far in the direction of aldehyde and **8**. Hydrogen gas proved to be an efficient trap for reactive intermediate **B**, and hydrogenation of benzaldehyde catalyzed by **8** occurred under very mild temperature and pressure conditions (22 °C, 2.5 atm of H_2) (Scheme 7).

Experimental Section

[2,5-Ph$_2$-3,4-Tol$_2$(η^5-C$_4$COH)]Ru(CO)(Cl)(PPh$_3$) (7). A solution of PPh_3 (458 mg, 1.75 mmol) and ruthenium chloride **6** (330 mg, 0.54 mmol) in THF (35 mL) was refluxed under N_2 for 4 days with a periodic nitrogen purge. Solvent was evaporated under reduced pressure, and the residual solid was recrystallized from THF/pentane (4:1) at −30 °C to afford orange crystals of **7** (413 mg, 91% yield). Slow evaporation of a THF/hexane solution yielded X-ray-quality crystals. While crystalline **7** is stable for extended periods in air, its solutions are air sensitive. ^{1}H NMR (360 MHz, CD_2Cl_2): δ 2.21 (s, CpTolCH_3), 3.48 (s, OH), 6.90−7.50 (m, aromatic). ^{13}C{^{1}H} NMR (90 MHz, CD_2Cl_2): δ 21.3 (CpTolCH_3); 21.5 (CpTolCH_3); 76.1, 86.0 (C 3,4 of Cp); 102.1, 105.1 (C 2,5 of Cp); 128−138 (31 resonances, aromatic); 137.6 (C1 of Cp); 206.8 (d, $J_{CP} = 18.1$ Hz, CO). ^{31}P{^{1}H} NMR (146 MHz, CD_2Cl_2) δ 46.5. IR (CH_2Cl_2): 1950 cm^{-1}. HRMS (ESI): calcd (found) for $[C_{50}H_{39}ClO_2PRu]^-$ 839.1420 (839.1416).

[2,5-Ph$_2$-3,4-Tol$_2$(η^5-C$_4$COH)]Ru(CO)(H)(PPh$_3$) (8). A degassed solution of **7** (250 mg, 0.297 mmol) and NaOMe (9 mL, 0.5 M) in MeOH was refluxed under N_2 for 4 h. After the mixture was cooled, a 5% HCl solution (7.5 mL) was added under a stream of N_2, leading to formation of an off-white precipitate. This suspension was extracted with toluene (3 × 10 mL), and the toluene extract was evaporated under vacuum to afford **8** (199 mg, 83% yield) as a pale yellow powder. Slow diffusion of pentane into a toluene solution of **8** at −30 °C gave bright yellow crystals suitable for X-ray crystallographic analysis. ^{1}H NMR (toluene-d_8, 300 MHz): δ −10.37 (d, $J_{HP} = 34.2$ Hz, RuH), 1.83 (s, CpTolCH_3), 1.89 (s, CpTolCH_3), 4.25 (s, OH), 6.63−7.54 (aromatic). ^{1}H NMR (300 MHz, C_6D_6): δ −10.07 (d, $J_{PH} = 34.5$ Hz, RuH), 1.80 (s, CpTolCH_3), 1.84 (s, CpTolCH_3), 3.28 (s, OH), 6.67−6.91 (m, 15H), 6.97−7.10 (m, 4H), 7.45−7.56 (m, 10H), 7.71 (m, 4H). ^{1}H NMR (300 MHz, CD_2Cl_2): −10.71 (d, $J_{PH} = 33.6$ Hz, RuH), 2.19 (s,

CpTolCH_3), 2.22 (s, CpTolCH_3), 3.20 (s, OH), 6.85 (d, J = 8.0 Hz, 2H), 6.90 (d, J = 7.7 Hz, 2H), 6.98 (m, 6H), 7.08 (m, 4H), 7.14−7.37 (m, 19 H). $^{13}C\{^1H\}$ NMR (90 MHz, C_6D_6): δ 21.3 (CpTol*C*H_3); 21.4 (CpTol*C*H_3); 88.8, 89.0 (C 3,4 of Cp); 103.4, 103.5 (C2,5 of Cp); 125−139 (31 resonances, aromatic); 137.1 (C1 of Cp); 208.4 (d, J_{CP} = 19 Hz, CO). $^{31}P\{^1H\}$ NMR (145 MHz, C_6D_6) δ 63.4. IR (CH_2Cl_2): 1918 cm^{-1}. HRMS (ESI): calcd (found) for $[C_{50}H_{40}O_2PRu]^-$ 805.1809 (805.1808).

[2,5-Ph$_2$-3,4-Tol$_2$(η^5-C$_4$COH)]Ru(O$_2$CPh)(PPh$_3$)(CO) (9). In an inert-atmosphere glovebox, a toluene solution of **8** (40.0 mg, 0.050 mmol) and benzaldehyde (0.40 mL, 3.94 mmol) was stirred at room temperature for 24 h. Solvent was evaporated under vacuum, and the residual solid was redissolved in toluene. Benzaldehyde (0.40 mL, 3.94 mmol) was added, and the solution was stirred for 24 h. Solvent was evaporated under vacuum, and the resulting solid was washed twice with pentane to afford **9** (29.9 mg, 65% yield) as a pale yellow solid. X-ray-quality crystals of **9** were obtained by recrystallization from toluene. ^1H NMR (toluene-d_8, 360 MHz): δ 1.61 (s, CpTolCH_3), 1.81 (s, CpTolCH_3), 3.88 (s, OH), 6.6−8.1 (38 H, aromatics). $^{13}C\{^1H\}$ NMR (THF-d_8, 125 MHz): δ 20.9, 22.0 (CpTol*C*H_3); 73.3, 85.5 (C3, 4 of Cp); 102.2, 105.5 (C2, 5 of Cp); 126−138 (24 resonances, Ar); 173.7 (Ph*C*O_2); 209.0 (d, J_{PC} = 20.4 Hz, CO). $^{31}P\{^1H\}$ NMR (toluene-d_8, 145 MHz): δ 52.4. IR (CH_2Cl_2): 1958 cm^{-1}. IR (toluene): 1960 cm^{-1}. HRMS (ESI): calcd (found) for $[C_{50}H_{40}O_2PRu]^+$ (**9**−O_2CPh)$^+$: 805.1809 (805.1819).

[2,5-Ph$_2$-3,4-Tol$_2$(η^5-C$_4$COH)]Ru(O$_2$CTol)(PPh$_3$)(CO) (9-Me). A solution of *p*-tolualdehyde (0.50 mL, 4.2 mmol) and **8** (50 mg, 0.062 mmol) in toluene (5 mL) was stirred for 24 h. The toluene was evaporated under vacuum, the residue was washed with pentane and redissolved in toluene, and *p*-tolualdehyde (0.50 mL, 4.2 mmol) was added. After an additional 24 h, toluene was evaporated and the residue was washed with pentane to give **9-Me** as a pale yellow powder. ^1H NMR (300 MHz, C_6D_6): δ 1.57 (s, 3H), 1.77 (s, 3H), 2.08 (s, 3H), 3.87 (s, 1H), 6.61−7.75 (m, 33H), 7.93 (d, J = 8.4 Hz, 2H), 8.09 (d, J = 8.4 Hz, 2H). ^1H NMR (500 MHz, CD_2Cl_2): δ 2.06 (s, 3H), 2.24 (s, 3H), 2.30 (s, 3H), 3.68 (s, 1H), 6.71 (d, J = 8.1 Hz, 2H), 6.89 (td, J = 7.7, 1.6 Hz, 6H), 6.97 (d, J = 8.1 Hz, 4H), 7.02−7.08 (m, 7H), 7.15−7.21 (m, 8H), 7.27−7.32 (m, 6H), 7.43−7.47 (m, 4H). $^{13}C\{^1H\}$ NMR (126 MHz, CD_2Cl_2): δ 21.3, 21.5, 21.6, 73.17, 85.3 (d, J_{PC} = 2 Hz), 102.1 (d, J_{PC} = 5 Hz), 104.9 (d, J_{PC} = 8 Hz), 127.4−134.4 (48C, 21 resonances), 137.4, 138.0, 140.1, 173.9, 208.6 (d, J_{PC} = 22 Hz). $^{31}P\{^1H\}$ NMR (203 MHz, CD_2Cl_2): δ 50.8. IR (CH_2Cl_2): 1953 cm^{-1}.

Alternatively, **9-Me** was prepared by combining **8** (10 mg, 12 μmol), *p*-tolualdehyde (13 μL, 11 μmol), and *p*-toluic acid (3.3 mg, 24 μmol) in benzene (0.9 mL). After 24 h, most of the **9-Me** had precipitated. After half of the benzene was evaporated under reduced pressure, the remaining liquid was decanted by pipet and the residue was washed with pentane to give **9-Me** (10.5 mg, 90%) as a pale yellow powder.

Exchange of Deuterium from 8-RuDOD into *p*-Tolualdehyde. Excess distilled *p*-tolualdehyde (15.2 μL, 129 μmol) was added to a solution of **8-RuDOD** (150 μL (0.0430 M solution in toluene-d_8), 6.45 μmol) in toluene-d_8 (0.45 mL), and the appearance of a hydride resonance of **8** (δ −10.37) was monitored by ^1H NMR spectroscopy at 26 °C over 140 min. Pseudo first-order appearance of the hydride resonance was observed.

Catalytic Hydrogenation of Benzaldehyde by 8 Monitored by NMR Spectroscopy. A solution of benzaldehyde (20 μL, 0.1 mmol, 0.526 M) and ruthenium hydride **8** (7.3 mg, 9.1 μmol, 18 mM) in 0.5 mL of toluene-d_8 in a resealable NMR tube was degassed by three freeze−pump−thaw cycles, cooled to −196 °C, and placed under 0.66 atm of H_2. Benzaldehyde disappearance (δ 9.59, aldehyde CH) and benzyl alcohol appearance (δ 4.30, CH_2OH) were followed by ^1H NMR spectroscopy at room temperature.

In Situ IR Spectroscopy Monitoring of Hydrogenation of Benzaldehyde Catalyzed by 8. This process will be illustrated with a specific example. A toluene solution (5.1 mL) containing benzaldehyde (0.5 mL, 4.9 mmol, 0.97 M) and **8** (25.0 mg, 0.031 mmol, 6.1 mM, 0.6 mol %) was prepared in a high-pressure vessel equipped with an attenuated total reflection element (ReactIR). The reaction vessel was heated to 45 °C under a nitrogen atmosphere. The vessel was flushed with H_2 three times, pressurized to 35 atm of H_2, and maintained at that pressure during the course of the hydrogenation. The hydrogenation of benzaldehyde was followed by measuring the intensity of the CO stretching frequency of benzaldehyde (1709 cm^{-1}) every 4 min.

Acknowledgment. Financial support from the Department of Energy, Office of Basic Energy Sciences, is gratefully acknowledged. J.B.J. thanks the ACS Organic Division Emmanuil Troyansky Graduate Fellowship for support. Grants from the NSF (No. CHE-962-9688) and NIH (No. I S10 RR04981-01) for the purchase of NMR spectrometers are acknowledged.

Supporting Information Available: Text, tables, and figures detailing measures of acidity of **7** and **8**, the disproportionation of benzaldehyde catalyzed by **8** and benzoic acid, the loss of H_2 from **8**, the PGSE NMR of **9**, the oxidation of benzyl alcohol by **9**, reactions of **9** and **9-Me** with H_2, the preparation of **11**, the preparation of **8-RuDOD**, catalytic hydrogenation of an imine by **8**, plots of rate vs pH_2, of rate vs [**8**], and of ln [ald] vs time for benzaldehyde hydrogenation by **8**, and X-ray crystal structure data (the corresponding CIF files are also given) for **7**−**9**. This material is available free of charge via the Internet at http://pubs.acs.org.

OM0509387